Ancestral process for infectious disease outbreaks with superspreading

Xavier Didelot[1,2,*], David Helekal[3], Ian Roberts[2]

[1] School of Life Sciences, University of Warwick, Coventry, United Kingdom

[2] Department of Statistics, University of Warwick, Coventry, United Kingdom

[3] Department of Immunology and Infectious Diseases, Harvard T. H. Chan School of Public Health, Boston, Massachusetts, USA

[*] Corresponding author. Tel: 0044 (0)2476 572827. Email: xavier.didelot@gmail.com

Running title: Ancestry for outbreaks with superspreading

Keywords: infectious disease epidemiology modelling; offspring distribution; superspreading; outbreaks; lambda-coalescent model; multiple mergers

Abstract

When an infectious disease outbreak is of a relatively small size, describing the ancestry of a sample of infected individuals is difficult because most ancestral models assume large population sizes. Given a set of infected individuals, we show that it is possible to express exactly the probability that they have the same infector, either inclusively (so that other individuals may have the same infector too) or exclusively (so that they may not). To compute these probabilities requires knowledge of the offspring distribution, which determines how many infections each infected individual causes. We consider transmission both without and with superspreading, in the form of a Poisson and a Negative-Binomial offspring distribution, respectively. We show how our results can be incorporated into a new lambda-coalescent model which allows multiple lineages to coalesce together. We call this new model the omega-coalescent, we compare it with previously proposed alternatives, and advocate its use in future studies of infectious disease outbreaks.

1 Introduction

An outbreak of an infectious disease typically starts when a single or a small number of infected individuals appear within a susceptible population. Each infected individual may come in contact and transmit the disease to each of the susceptible individuals, who will then become infected in their turn and spread the disease further. Most mathematical models of infectious diseases describe situations where the disease is at an equilibrium, when the number of infected individuals is high and/or with a significant part of the population already infected (Anderson and May 1991; Keeling and Rohani 2008). Here however we focus on the early stages of an epidemic, where the number of infected individuals is small and the number of susceptibles comparatively high and constant. In this situation it is useful to consider the number of new infections that each infected individual is likely to cause, and the probabilistic distribution for this number is often called the offspring distribution (Grassly and Fraser 2008). The mean of the offspring distribution is called the basic reproduction number R_0 and has been given much attention especially since it determines how likely the outbreak is to spread, and how much effort would be needed to bring it under control (Fraser et al. 2004; Ferguson et al. 2006).

If we consider that all individuals are infectious for the same duration and with the same transmission rate, the offspring distribution is Poisson distributed with mean R_0, in which case the variance of the offspring distribution is also R_0. We would then say that there is no transmission heterogeneity. However, in practice there are many reasons why this may not be the case, with some individuals being infectious for longer than others, or being more infectious than others, or having more frequent contacts with susceptibles, or being less symptomatic and therefore less likely to reduce contact numbers, etc. All these factors cause the offspring distribution to be more dispersed than it would otherwise be, that is to have a variance greater than its mean R_0. A frequent choice to capture this overdispersion is to model the offspring distribution using a Negative-Binomial distribution with mean R_0 and dispersion parameter r (Lloyd-Smith et al. 2005; Grassly and Fraser 2008). When r is close to zero the variance is high compared to the mean, whereas when r is high the variance becomes close to the mean. This transmission heterogeneity is often called superspreading, although this is perhaps misleading as it is the rule rather than the exception of how infectious diseases spread. Superspreading has indeed been described in many diseases (Woolhouse et al. 1997; Stein 2011; Kucharski and Althaus 2015; Wang et al. 2021), and most recently for SARS-CoV-2 (Wang et al. 2020; Lemieux et al. 2021; Gómez-Carballa et al. 2021; Du et al. 2022).

As an outbreak unfolds forward-in-time, a transmission tree is generated representing who-infected-whom, in which each node is an infected individual and points towards a number of nodes distributed

according to the offspring distribution. Here we consider the reverse problem of the transmission ancestry, going backward-in-time, from a sample of infected individuals, until reaching the last common transmission ancestor of the whole sample. Given a set of n sampled individuals, we show how to calculate the probability that a given subset of size k have the same infector, either inclusively (so that the remaining $n-k$ may also have the same infector or not) or exclusively (so that none of the remaining $n-k$ have the same infector). We start by considering the general case of an offspring distribution with arbitrary form, and then the specific cases of offspring distributions that follow a Poisson and a Negative-Binomial distribution. The main novelty of our approach is that we consider that the overall population size is small, but we show that in the limit where the population size is large, our results agree with several previous studies (Volz 2012; Koelle and Rasmussen 2012; Fraser and Li 2017). Finally, we show how our results can be incorporated into a new lambda-coalescent model (Pitman 1999; Sagitov 1999; Donnelly and Kurtz 1999) and compare it with previously proposed models.

2 General offspring distribution case

Let time be measured in discrete units and denoted t. Each discrete value of t corresponds to a unique non-overlapping generation of infected individuals, so that individuals infected at t have offspring at $t+1$, etc. Let N_t denote the number of infectious individuals at time t. Each of them creates a number $s_{t,i}$ of secondary infections at time $t+1$, following the offspring distribution $\alpha_t(s)$. The mean of this distribution is the basic reproduction number R_t and the variance is V_t. The total number of infected individuals at time $t+1$ is given by:

$$N_{t+1} = \sum_{i=1}^{N_t} s_{t,i} \tag{1}$$

2.1 Inclusive coalescence probability

We define the inclusive coalescence probability $p_{k,t}(N_t, N_{t+1})$ as the probability that a specific set of k individuals from generation $t+1$ have the same infector in generation t, conditional on population sizes N_t and N_{t+1}. Given full information about offspring counts from individuals in generation t, $\mathbf{s}_t = (s_{t,1}, \dots s_{t,N_t})$, we have:

$$
\begin{aligned}
p_{k,t}(\mathbf{s}_t, N_t) &= \sum_{i=1}^{N_t} \frac{\binom{s_{t,i}}{k}}{\binom{N_{t+1}}{k}} \\
&= \sum_{i=1}^{N_t} \frac{s_{t,i}!}{(s_{t,i}-k)!} \frac{(N_{t+1}-k)!}{N_{t+1}!}
\end{aligned} \tag{2}
$$

Full information $\{s_{t,i}\}$ yields the population size N_{t+1} as shown in Equation 1, but this is not available in practice. We can instead express the inclusive coalescence probability conditioning on the next population size N_{t+1} by summing over possible offspring counts $\mathbf{s}_t = (s_{t,1}, \dots s_{t,N_t})$ conditional on the total generation size. Let $S_t^{-(1)} = (S_{t,2}, \dots, S_{t,N_t})$:

$$
\begin{aligned}
p_{k,t}(N_t, N_{t+1}) &= \sum_{\mathbf{s}_t \in \mathbb{N}_0^{N_t}} \mathbb{P}\left[\mathbf{S}_t = \mathbf{s}_t \middle| \sum_{i=1}^{N_t} S_{t,i} = N_{t+1}\right] p_{k,t}(\mathbf{s}_t, N_t) \\
&= \sum_{\mathbf{s}_t \in \mathbb{N}_0^{N_t}} \mathbb{P}\left[\mathbf{S}_t = \mathbf{s}_t \middle| \sum_{i=1}^{N_t} S_{t,i} = N_{t+1}\right] \sum_{i=1}^{N_t} \frac{\binom{s_{t,i}}{k}}{\binom{N_{t+1}}{k}} \\
&= \sum_{i=1}^{N_t} \sum_{\mathbf{s}_t \in \mathbb{N}_0^{N_t}} \frac{\binom{s_{t,i}}{k}}{\binom{N_{t+1}}{k}} \mathbb{P}\left[S_{t,1} = s_{t,1}, \mathbf{S}_t^{-(1)} = \mathbf{s}_t^{-(1)} \middle| \sum_{i=1}^{N_t} S_{t,i} = N_{t+1}\right] \\
&= \frac{N_t}{\binom{N_{t+1}}{k}} \sum_{\mathbf{s}_t \in \mathbb{N}_0^{N_t}} \binom{s_{t,1}}{k} \mathbb{P}\left[S_{t,1} = s_{t,1} \middle| \sum_{i=1}^{N_t} S_{t,i} = N_{t+1}\right] \\
&\qquad \times \mathbb{P}\left[\mathbf{S}_t^{-(1)} = \mathbf{s}_t^{-(1)} \middle| S_{t,1} = s_{t,1}, \sum_{i=1}^{N_t} S_{t,i} = N_{t+1}\right] \\
&= \frac{N_t}{\binom{N_{t+1}}{k}} \sum_{s_{t,1}=0}^{N_{t+1}} \binom{s_{t,1}}{k} \mathbb{P}\left[S_{t,1} = s_{t,1} \middle| \sum_{i=1}^{N_t} S_{t,i} = N_{t+1}\right] \\
&\qquad \times \underbrace{\sum_{\mathbf{s}_t^{-(1)} \in \mathbb{N}_0^{N_t - 1}} \mathbb{P}\left[\mathbf{S}_t^{-(1)} = \mathbf{s}_t^{-(1)} \middle| \sum_{i=2}^{N_t} S_{t,i} = N_{t+1} - s_{1,t}\right]}_{=1} \\
&= \frac{N_t}{\binom{N_{t+1}}{k}} \mathbb{E}\left[\binom{S_{t,1}}{k} \middle| \sum_{i=1}^{N_t} S_{t,i} = N_{t+1}\right] \\
&= N_t \frac{(N_{t+1}-k)!}{N_{t+1}!} \mathbb{E}\left[\frac{S_{t,1}!}{(S_{t,1}-k)!} \middle| \sum_{i=1}^{N_t} S_{t,i} = N_{t+1}\right]
\end{aligned} \tag{3}
$$

The k-th falling factorial moments $\mathbb{E}\big[\frac{S_{t,1}!}{(S_{t,1}-k)!}\big|\sum_{i=1}^{N_t} S_{t,i} = N_{t+1}\big]$ in Equation 3 can be readily obtained by differentiating the probability generating function of $S_{t,1}|(\sum_{i=1}^{N_t} S_{t,i} = N_{t+1})$.

2.2 Exclusive coalescence probability

Generally, we observe a sample of individuals from each generation rather than the entire population. In this case, we are interested in the exclusive coalescence probability $p_{n,k,t}(N_t, N_{t+1})$ that a specific subset of k individuals amongst n sampled individuals arose from a common infector one generation in the past given knowledge of the total population sizes N_t and N_{t+1}. Let us first assume full knowledge about offspring counts of the individuals at time N_t amongst the sample at time N_{t+1}, namely $\mathbf{x}_t = (x_{t,1}, \ldots, x_{t,N_t})$ such that $x_{t,1} + ... + x_{t,N_t} = n$. Note that $X_{t,i}$ does not follow the same offspring distribution as $S_{t,i}$. We have:

$$\begin{aligned} p_{n,k,t}(\mathbf{x}_t, N_t) &= \sum_{i=1}^{N_t} \frac{\binom{x_{t,i}}{k}}{\binom{n}{k}} \mathbb{I}\{x_{t,i} = k\} \\ &= \sum_{i=1}^{N_t} \frac{x_{t,i}!}{(x_{t,i}-k)!} \frac{(n-k)!}{n!} \mathbb{I}\{x_{t,i} = k\} \end{aligned} \tag{4}$$

Similarly to the inclusive coalescence probability in Equation 3, we can use this to evaluate the exclusive probability given N_t and N_{t+1} by summing over possible parent offspring configurations (for $k \leq n$):

$$\begin{aligned} p_{n,k,t}(N_t, N_{t+1}) &= \sum_{\mathbf{x}_t \in \mathbb{N}_0^{N_t}} \mathbb{P}\left[\mathbf{X}_t = \mathbf{x}_t \middle| \sum_{i=1}^{n} X_{t,i} = n\right] p_{n,k,t}(\mathbf{x}_t, N_t) \\ &= \sum_{\mathbf{x}_t \in \mathbb{N}_0^{N_t}} \mathbb{P}\left[\mathbf{X}_t = \mathbf{x}_t \middle| \sum_{i=1}^{n} X_{t,i} = n\right] \sum_{i=1}^{N_t} \frac{\binom{x_{t,i}}{k}}{\binom{n}{k}} \mathbb{I}\{x_{t,i} = k\} \\ &= \frac{N_t}{\binom{n}{k}} \sum_{\mathbf{x}_t \in \mathbb{N}_0^{N_t}} \binom{x_{t,1}}{k} \mathbb{P}\left[\mathbf{X}_t = \mathbf{x}_t \middle| \sum_{i=1}^{N_t} X_{t,i} = n\right] \mathbb{I}\{x_{t,1} = k\} \\ &= \frac{N_t}{\binom{n}{k}} \sum_{\mathbf{x}_t^{-(1)} \in \mathbb{N}_0^{N_t - 1}} \binom{k}{k} \mathbb{P}\left[X_{t,1} = k, \mathbf{X}_t^{-(1)} = \mathbf{x}_t^{-(1)} \middle| \sum_{i=1}^{N_t} X_{t,i} = n\right] \\ &= \frac{N_t}{\binom{n}{k}} \mathbb{P}[X_{t,1} = k \Big| \sum_{i=1}^{N_t} X_{t,i} = n] \underbrace{\sum_{\mathbf{x}_t^{-(1)} \in \mathbb{N}_0^{N_t - 1}} \mathbb{P}\left[\mathbf{X}_t^{-(1)} = \mathbf{x}_t^{-(1)} \middle| \sum_{i=1}^{N_t} X_{t,i} = n, X_{t,1} = k\right]}_{=1} \end{aligned}$$

$$= \frac{N_t}{\binom{n}{k}} \mathbb{P}\left[X_{t,1} = k \middle| \sum_{i=1}^{N_t} X_{t,i} = n \right] \tag{5}$$

2.3 Complementarity of exclusive coalescence probabilities

If we consider one of the lines observed amongst a set of n, it can either remain uncoalesced with probability $p_{n,1,t}(N_t, N_{t+1})$ or coalesce in an event of size k with probability $p_{n,k,t}(N_t, N_{t+1})$ with any set of $k-1$ lines among the $n-1$ other lines, leading to the following complementarity equation:

$$\sum_{k=1}^{n} \binom{n-1}{k-1} p_{n,k,t}(N_t, N_{t+1}) = 1 \tag{6}$$

We can show that it is indeed satisfied by the formula in Equation 5:

$$\begin{aligned}
\sum_{k=1}^{n} \binom{n-1}{k-1} p_{n,k,t}(N_t, N_{t+1}) &= \sum_{k=1}^{n} \binom{n-1}{k-1} \frac{N_t}{\binom{n}{k}} \mathbb{P}\left[X_1 = k \middle| \sum_{i=1}^{N_t} X_i = n \right] \\
&= \sum_{k=1}^{n} N_t \frac{k}{n} \mathbb{P}\left[X_1 = k \middle| \sum_{i=1}^{N_t} X_i = n \right] \\
&= \frac{N_t}{n} \sum_{k=0}^{n} k \mathbb{P}\left[X_1 = k \middle| \sum_{i=1}^{N_t} X_i = n \right] \\
&= \frac{N_t}{n} \mathbb{E}\left[X_1 \middle| \sum_{i=1}^{N_t} X_i = n \right] \\
&= \frac{1}{n} \sum_{i=1}^{N_t} \mathbb{E}\left[X_i \middle| \sum_{i=1}^{N_t} X_i = n \right] \\
&= \frac{1}{n} \mathbb{E}\left[\sum_{i=1}^{N_t} X_i \middle| \sum_{i=1}^{N_t} X_i = n \right] \\
&= 1
\end{aligned} \tag{7}$$

3 Poisson offspring distribution case

In this section we consider that the offspring distribution is $\alpha_t = \text{Poisson}(R_t)$. In this case, we have:

$$\sum_{i=1}^{N_t} S_{t,i} \sim \text{Poisson}(N_t R_t) \tag{8}$$

and the conditional distribution:

$$\begin{aligned}
\mathbb{P}\left[S_{t,1} = s \middle| \sum_{i=1}^{N_t} S_{t,i} = N_{t+1}\right] &= \frac{\mathbb{P}\left[S_{t,1} = s, \sum_{i=1}^{N_t} S_{t,i} = N_{t+1}\right]}{\mathbb{P}\left[\sum_{i=1}^{N_t} S_{t,i} = N_{t+1}\right]} \\
&= \frac{\alpha_t(s)\,\mathbb{P}\left[\sum_{i=2}^{N_t} S_{t,i} = N_{t+1} - s\right]}{\mathbb{P}\left[\sum_{i=1}^{N_t} S_{t,i} = N_{t+1}\right]} \\
&= \frac{\frac{R_t^s e^{-R_t}}{s!} \cdot \frac{((N_t-1)R_t)^{N_{t+1}-s}}{(N_{t+1}-s)!}}{\frac{(N_t R_t)^{N_{t+1}} e^{-N_t R_t}}{N_{t+1}!}} \\
&= \binom{N_{t+1}}{s} \left(\frac{1}{N_t}\right)^s \left(1 - \frac{1}{N_t}\right)^{N_{t+1}-s}
\end{aligned} \tag{9}$$

This is the probability mass function of a Binomial distribution and therefore we deduce that:

$$S_{t,1} \middle| \left(\sum_{i=1}^{N_t} S_{t,i} = N_{t+1}\right) \sim \text{Binomial}\left(N_{t+1}, \frac{1}{N_t}\right) \tag{10}$$

The k-th falling factorial moments of $X \sim \text{Binomial}(n, p)$ are (Potts 1953):

$$\mathbb{E}\left[\frac{X!}{(X-k)!}\right] = \binom{n}{k} p^k k! \tag{11}$$

By applying this formula to the Binomial distribution in Equation 10 and injecting into Equation 3, we deduce that the inclusive probability of coalescence for k lines is:

$$p_{k,t}(N_t, N_{t+1}) = \frac{1}{N_t^{k-1}} \tag{12}$$

In addition, following a similar reasoning as for Equation 10 we can show that:

$$X_{t,1} \Big| \left(\sum_{i=1}^{N_t} X_{t,i} = n \right) \sim \text{Binomial}\left(n, \frac{1}{N_t} \right) \tag{13}$$

By injecting the probability mass function of this Binomial distribution into Equation 5 we deduce that the exclusive probability of coalescence for k lines from a sample of n ($n \geq k$) is:

$$p_{n,k,t}(N_t, N_{t+1}) = \frac{(N_t - 1)^{n-k}}{N_t^{n-1}} \tag{14}$$

It is interesting to note that neither the inclusive nor the exclusive coalescence probability depend on the mean R_t of the Poisson offspring distribution or the size N_{t+1} of the population at time $t+1$. Both only depend on the population size N_t at time t. The inclusive coalescent probability in Equation 12 can also be obtained conceptually by considering that among the k lines, the first one has an ancestor with probability one, and the remaining $k-1$ need to have the same ancestor among a set of N_t from which they choose uniformly at random so that the probability of picking the same ancestor is $1/N_t$. The exclusive coalescent probability in Equation 14 can be derived likewise by considering that in addition to the above, each of the $n-k$ other lines need to choose a different ancestor, which happens with probability $(N_t - 1)/N_t$. Figure 1 illustrates the inclusive and exclusive coalescence probabilities for a set of size $k = 1$ to $k = 10$ amongst a total of $n = 10$ observed individuals, in a population of size $N_t = 10$, $N_t = 20$ or $N_t = 30$.

4 Negative-Binomial offspring distribution case

In this section we consider that the offspring distribution is α_t = Negative-Binomial(r, p) with parameters (r, p) set by moment-matching the mean R_t and variance V_t of the offspring distribution which are assumed constant over time. The resulting parameters for this distribution are r =

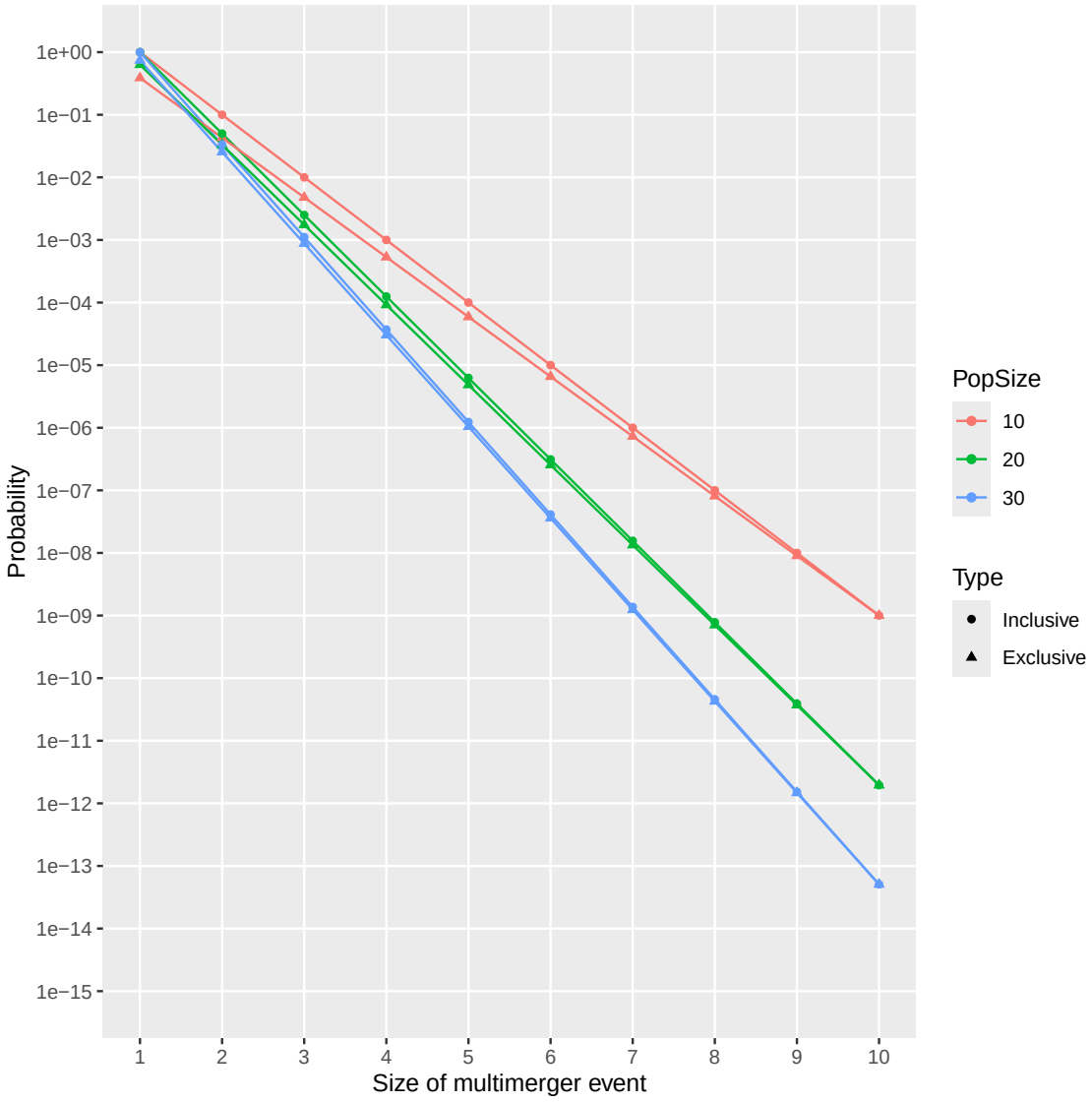

Figure 1: Inclusive and exclusive coalescence probabilities for the Poisson case.

$R_t^2/(V_t - R_t)$ and $p = R_t/V_t$. In this case, we have:

$$\sum_{i=1}^{N_t} S_{t,i} \sim \text{Negative-Binomial}(N_t r, p) \tag{15}$$

and similarly to the Poisson offspring distribution case we identify that the conditional distribution of $S_{t,1} | \sum_{i=1}^{N_t} S_{t,i}$ is as follows:

$$\begin{aligned}
\mathbb{P}\left[S_{t,1} = s \middle| \sum_{i=1}^{N_t} S_{t,i} = N_{t+1}\right] &= \frac{\alpha_t(s) \cdot \mathbb{P}\left[\sum_{i=2}^{N_t} S_{t,i} = N_{t+1} - s\right]}{\mathbb{P}\left[\sum_{i=1}^{N_t} S_{t,i} = N_{t+1}\right]} \\
&= \frac{\frac{\Gamma(r+s)}{s!\Gamma(r)}(1-p)^s p^r \cdot \frac{\Gamma\big((N_t-1)r + (N_{t+1}-s)\big)}{(N_{t+1}-s)!\Gamma((N_t-1)r)}(1-p)^{N_{t+1}-s} p^{(N_t-1)r}}{\frac{\Gamma(N_t r + N_{t+1})}{N_{t+1}!\Gamma(N_t r)}(1-p)^{N_{t+1}} p^{N_t r}} \\
&= \frac{N_{t+1}!}{s!(N_{t+1}-s)!} \frac{\Gamma(r+s)\Gamma\big((N_t-1)r + (N_{t+1}-s)\big)}{\Gamma(N_t r + N_{t+1})} \frac{\Gamma(N_t r)}{\Gamma(r)\Gamma\big((N_t-1)r\big)} \\
&= \binom{N_{t+1}}{s} \frac{\mathrm{B}(s+r, N_{t+1}-s+(N_t-1)r)}{\mathrm{B}(r,(N_t-1)r)}
\end{aligned} \tag{16}$$

where $\mathrm{B}(x,y)$ denotes the Beta function defined as $\mathrm{B}(x,y) = \Gamma(x)\Gamma(y)/\Gamma(x+y)$. This is the probability mass function of a Beta-Binomial distribution and therefore we deduce that:

$$S_{t,1} \left| \left(\sum_{i=1}^{N_t} S_{t,i} = N_{t+1} \right) \right. \sim \text{Beta-Binomial}(N_{t+1}, r, (N_t - 1)r) \tag{17}$$

The k-th falling factorial moments of $X \sim \text{Beta-Binomial}(n, \alpha, \beta)$ are (Tripathi et al. 1994):

$$\mathbb{E}\left[\frac{X!}{(X-k)!}\right] = \binom{n}{k} \frac{\mathrm{B}(\alpha+k, \beta)k!}{\mathrm{B}(\alpha,\beta)} \tag{18}$$

By applying this formula to the Beta-Binomial distribution in Equation 17 and injecting into Equation 3, we deduce that the inclusive probability of coalescence for k lines is:

$$p_{k,t}(N_t, N_{t+1}) = \frac{\mathrm{B}(N_t r + 1, r + k)}{\mathrm{B}(r + 1, N_t r + k)} \tag{19}$$

In addition, following a similar reasoning as for Equation 17, we can show that:

$$X_{t,1} \Bigg| \left(\sum_{i=1}^{N_t} X_{t,i} = n \right) \sim \text{Beta-Binomial}(n, r, (N_t - 1)r) \tag{20}$$

By injecting the probability mass function of this Beta-Binomial distribution into Equation 5 we deduce that the exclusive probability of coalescence for k lines is:

$$p_{n,k,t}(N_t, N_{t+1}) = \frac{N_t \mathrm{B}(k + r, n - k + N_t r - r)}{\mathrm{B}(r, N_t r - r)} \tag{21}$$

It is interesting to note that as for the Poisson case, the inclusive and exclusive coalescence probabilities do not depend on the size N_{t+1} of the population at time $t + 1$. They both depend on the Negative-Binomial offspring distribution only through the dispersion parameter r. If we consider that r is large in Equations 19 and 21, we can derive that the asymptotic behaviour is the same as in the Poisson case shown in Equations 12 and 14. For example this can be derived by rewriting the Beta functions using Gamma functions, and using the following form of Stirling's approximation:

$$\lim_{a \to \infty} \frac{\Gamma(a + b)}{\Gamma(a)} = a^b \mathrm{e}^{-b} \tag{22}$$

Figure 2 illustrates the inclusive and exclusive coalescence probabilities for the Negative-Binomial case for a set of size $k = 1$ to $k = 10$ amongst a total of $n = 10$ observed lines, in a population with size $N_t = 20$. Several Negative-Binomial offspring distributions are compared, all of which have the same mean $R_t = 2$, and with the dispersion parameter equal to $r = 0.1$, $r = 1$, $r = 10$ and $r = 100$ (Figure 2A). When $r = 1$ the Negative-Binomial reduces to a Geometric distribution. When r is high the dispersion is low and the Negative-Binomial case behaves almost like the Poisson case for both the inclusive (Figure 2B) and the exclusive coalescence probabilities (Figure 2C). When r is lower the dispersion of the offspring distribution increases, so that both the inclusive and exclusive probabilities of larger multimerger events are increased compared to the Poisson case. In particular, when $r = 0.1$ we see that the exclusive probability can increase with the size of the event considered (Figure 2C).

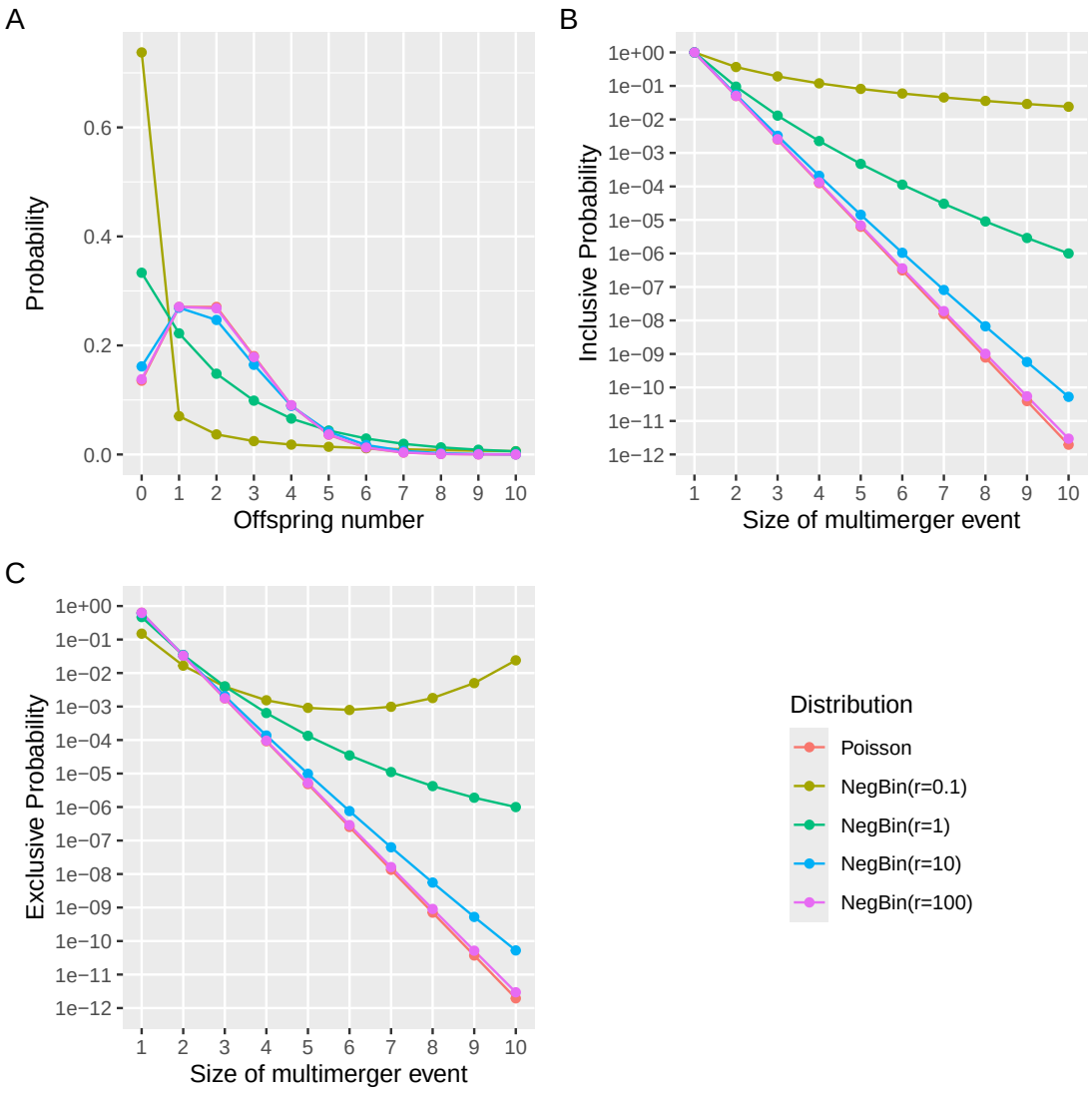

Figure 2: (A) Offspring distributions with mean $R_t = 2$. (B) Inclusive probability of coalescence for $N_t = 20$ and $n = 10$. (C) Exclusive probability of coalescence for $N_t = 20$ and $n = 10$.

This happens because the probability is not much lower for the common ancestor having say 10 rather than 9 offspring, while on the other hand if the event is of size 9 only then another individual in the generation of the ancestor needs to have had at least one sampled offspring.

5 Limit when the population size is large

If we consider that the population size N_t is fixed and large, we can show the connections between our results and several previous studies on the ancestral process of infectious diseases. In the Poisson case, from Equations 12 and 14 we can see that both inclusive and exclusive probabilities are of order $\mathcal{O}(N_t^{1-k})$. We can therefore ignore events with $k > 2$ and retain only the events with $k = 2$ which occur with the same inclusive and exclusive probabilities:

$$p_{2,t}(N_t, N_{t+1}) = p_{n,2,t}(N_t, N_{t+1}) = \frac{1}{N_t} \tag{23}$$

For the Negative-Binomial case, from Equations 19 and 21 we can rewrite using Gamma functions and apply the form of Stirling's equation given in Equation 22 to show that once again both inclusive and exclusive probabilities are also of order $\mathcal{O}(N_t^{1-k})$. We can therefore once again ignore events with $k > 2$ and retain only the events with $k = 2$ which occur with the same inclusive and exclusive probabilities:

$$p_{2,t}(N_t, N_{t+1}) = p_{n,2,t}(N_t, N_{t+1}) = \frac{r+1}{N_t r + 1} \approx \frac{r+1}{N_t r} \tag{24}$$

Koelle and Rasmussen (2012) derived the rates of coalescence of two lineages for several epidemiological models, assuming a large population at equilibrium. For each model they use the equation $N_\mathrm{e} = N/\sigma^2$ to relate the effective population size N_e to the actual population size N and the variance σ^2 in the number of offspring. This relationship was first established by Kingman (1982a) to derive the backward-in-time coalescent model from the forward-in-time Cannings exchangeable models (Cannings 1974). This result implies that the rate of coalescence for two lineages is $1/N_\mathrm{e} = \sigma^2/N$. From Equation 24 we can take $R_t = 1$ to achieve equilibrium of the population size and the method of moments estimator $r = R_t^2/(V_t - R_t) = 1/(V_t - 1)$ to deduce the equivalent result $p_{2,t}(N_t, N_{t+1}) = V_t/N_t$.

Volz (2012) showed that the rate of coalescence for two lineages under a continuous-time epidemic coalescent model is $2f(t)/I(t)^2$ where $f(t)$ is the incidence of the disease and $I(t)$ its prevalence. Setting

in this formula the prevalence as $I(t) = N_{t+1} = N_t R_t$ and the incidence as $f(t) = R_t I(t) = R_t^2 N_t$ we get a coalescent rate of $2/N_t$. To apply our methodology we need to consider that the offspring distribution is Geometric, since the epidemiological models considered have successes (transmission) happening until the first failure (removal). We therefore set $r = 1$ in Equation 24 to make the Negative-Binomial offspring distribution reduce to a Geometric distribution and the same result follows.

Fraser and Li (2017) calculated the effective population size $N_e(t)$ as a function of the actual population size $N(t)$ and the mean and variance of the offspring distribution R and σ^2. This formula was used to estimate the dispersion parameter of a Negative-Binomial offspring distribution from genetic data (Li et al. 2017). Using our notations, their formula is equivalent to the inclusive coalescence probability for two lineages:

$$p_{2,t}(N_t, N_{t+1}) = \frac{V_t/R_t + R_t - 1}{N_t R_t} \tag{25}$$

In the Poisson case we have $V_t = R_t$ so that Equation 25 simplifies to $1/N_t$ which agrees with Equation 23. In the Negative-Binomial case we have $V_t/R_t = 1/p = 1 + R_t/r$ so that Equation 25 simplifies to $(r+1)/(N_t r)$ which agrees with our Equation 24. Conversely, if we substitute the method of moments estimator $r = R_t^2/(V_t - R_t)$ in Equation 24 we obtain the Equation 25.

6 Definition of a new lambda-coalescent model

The coalescent model (Kingman 1982a,b) describes the ancestry of a sample from a large population evolving according to many forward-in-time models such as the Wright-Fisher model (Wright 1931; Fisher 1930), the Moran model (Moran 1958) and the Cannings exchangeable model (Cannings 1974). Since the coalescent considers a large population in which each individual only has a number of offspring that is small compared to the population size, coalescent trees are always binary and do not feature multimergers, making them unsuitable to represent the ancestry of outbreaks considered in this study. However, the lambda-coalescent model is an extension of the coalescent model that allows multimergers (Pitman 1999; Sagitov 1999; Donnelly and Kurtz 1999).

A lambda-coalescent model is defined by a probability measure $\Lambda(\mathrm{d}x)$ on the interval $[0, 1]$, from which we deduce the rate $\lambda_{n,k}$ at which any subset of k lineages within a set of n observed lineages coalesce:

$$\lambda_{n,k} = \int_0^1 x^{k-2}(1-x)^{n-k}\,\Lambda(\mathrm{d}x) \tag{26}$$

The beta-coalescent (Schweinsberg 2003) is a specific type of lambda-coalescent that has been used recently in several studies analysing genetic data from infectious disease agents (Hoscheit and Pybus 2019; Menardo et al. 2021; Helekal et al. 2025; Zhang and Palacios 2024). The beta-coalescent model has a single parameter $\alpha \in [0, 2]$ and is defined as:

$$\Lambda(\mathrm{d}x) = \frac{x^{1-\alpha}(1-x)^{\alpha-1}}{\mathrm{B}(2-\alpha, \alpha)}\mathrm{d}x \tag{27}$$

By combining Equations 26 and 27 we deduce that:

$$\lambda_{n,k} = \frac{\mathrm{B}(k-\alpha, n-k+\alpha)}{\mathrm{B}(2-\alpha, \alpha)} \tag{28}$$

Special cases of the beta-coalescent include $\alpha = 2$ corresponding to the Kingman coalescent, $\alpha = 1$ which is known as the Bolthausen-Sznitman coalescent and $\alpha = 0$ for which the phylogeny is always star-shaped.

We now define a new lambda-coalescent based on the Negative-Binomial case described previously. We call this new lambda-coalescent model the omega-coalescent (where omega stands for outbreak). For ease of comparison with other coalescent models, we consider that time is continuous and that the population size remains constant equal to N_t. The exclusive coalescent probability $p_{n,k,t}(N_t, N_{t+1})$ in the Negative-Binomial case given by Equation 21 can be used to determine the corresponding rate of the omega-coalescent, if we consider that the probability of each event in discrete time is the result of the event happening at a constant rate in continuous time:

$$\lambda_{n,k} = -\log(1 - p_{n,k,t}(N_t, N_{t+1})) \tag{29}$$

Note that this equation implies that time is measured continuously in number of transmission generations. For example to measure time in decimal days instead, the time scale would need to be multiplied by the mean of the generation time distribution measured in days (Svensson 2007). The omega-coalescent has two parameters: the constant population size N_t and the dispersion parameter

r. In order to compare the omega-coalescent defined in Equation 29 with other models such as the beta-coalescent defined in Equation 28, we consider the distribution of the size k of the next event among a set of n lineages. For any lambda-coalescent this can be computed as:

$$p(k|n) = \frac{\binom{n}{k}\lambda_{n,k}}{\sum_{i=2}^{n}\binom{n}{i}\lambda_{n,i}} \tag{30}$$

Figure 3 compares this distribution for $n = 10$ in the beta-coalescent with parameter $\alpha \in \{0.5, 1, 1.5\}$ and for the omega-coalescent with parameters $N_t \in \{10, 20, 30\}$ and $r \in \{0.1, 1, 10\}$. In the beta-coalescent, the distribution shifts towards more larger multimerger events as the parameter α decreases. In the omega-coalescent a wider range of behaviours is obtained when varying the two parameters N_t and r. For a given value of N_t, decreasing the value of r results in more larger events. Conversely, for a given value of r we can see that increasing the value of N_t reduces the probability of larger events.

Genealogies can be simulation from the omega-coalescent model defined in Equation 29 using the same algorithm as for other lambda-coalescent models (Pitman 1999). Figure 4 shows examples of trees simulated for a sample of size $n = 20$, constant population size $N_t = 30$ and dispersion parameter $r \in \{0.1, 1, 10, 100\}$. It is already clear from these single realisations that the lower values of r result in trees with more larger multimerger events and lower time to the most recent common ancestor, but to quantify these properties we need to consider many trees. Figure 5 shows summary statistics for 10,000 trees simulated in the same conditions as the individual trees shown in Figure 4. As the dispersion parameter increases from $r = 0.1$ to $r = 100$ multimerger events become less and less likely and less large (Figure 5A and B), and the time to the most recent common ancestor increases (Figure 5C). Furthermore, the stemminess of the tree increases, which is defined as the sum of lengths of internal branches divided by the total sum of branch lengths (Figure 5D). Stemminess is usually taken as a sign of population size dynamics (Fiala and Sokal 1985; Didelot et al. 2009), which would be misleading here since all simulations assumed a constant population size.

7 Parameter inference

Let us now consider a genealogy T with n leaves and c coalescent nodes, with $t_0 = 0$ the sampling time, $t_1, ..., t_c$ the times of the coalescent nodes in increasing order and k_i the number of lineages coalescing at time t_i. The number of lineages existing between time t_{i-1} and t_i is then $n_i = n - \sum_{j=1}^{i-1} k_j$. Under

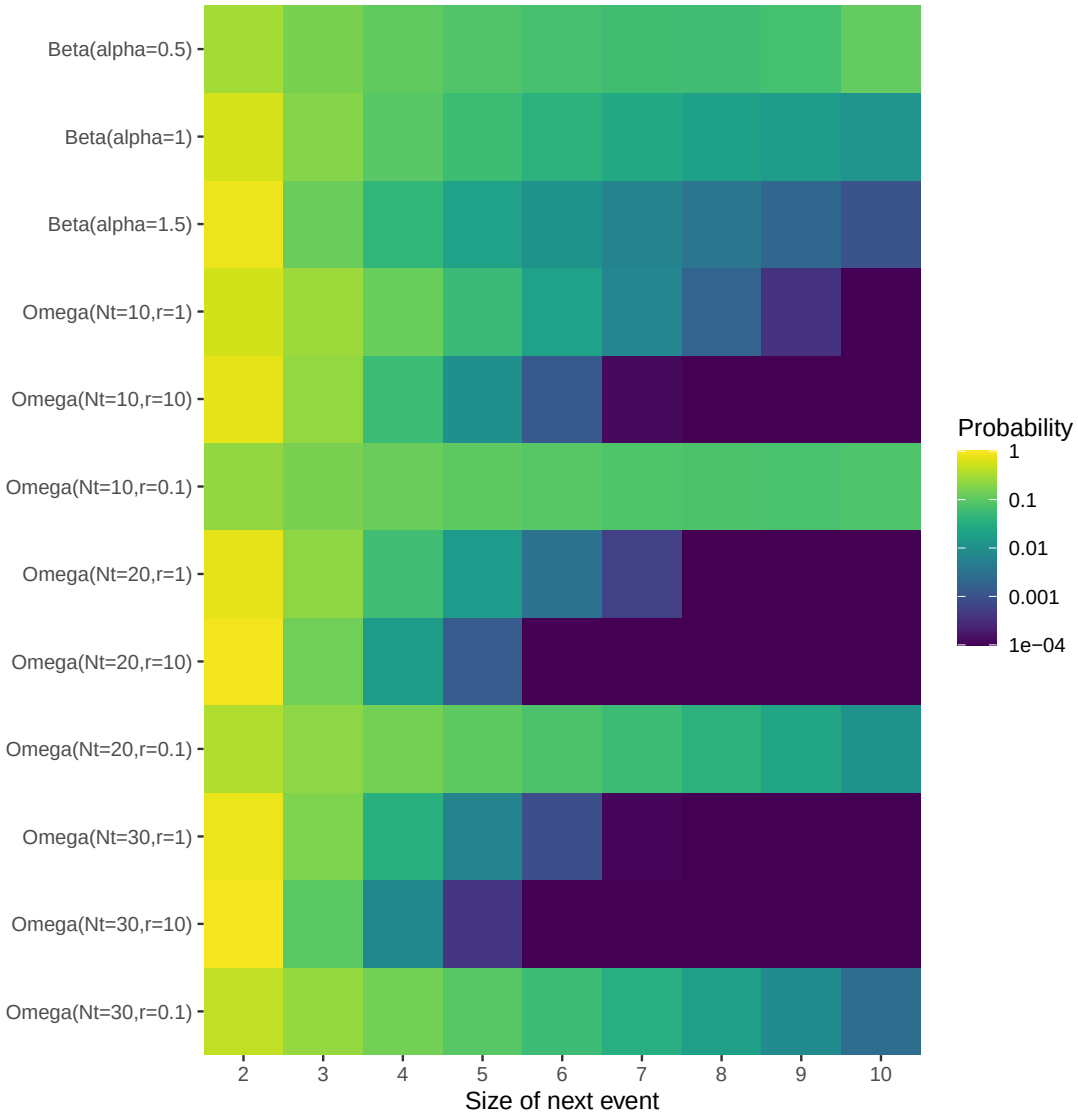

Figure 3: Distribution of the size of the next event among a set of $n = 10$ lineages, compared between the beta-coalescent and the omega-coalescent model with various parameters.

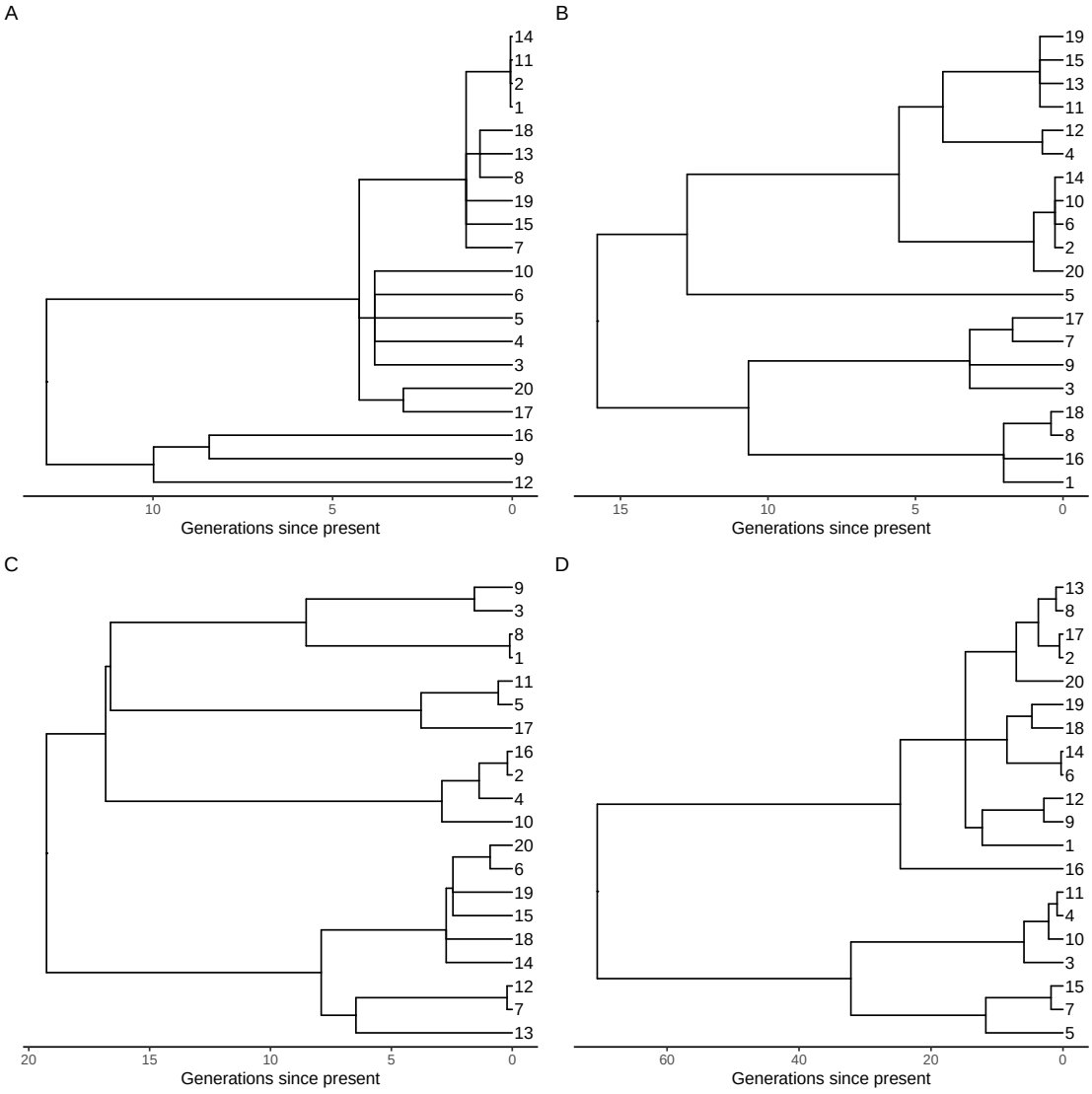

Figure 4: Example of trees simulated under the omega-coalescent with $r = 0.1$ (A), $r = 1$ (B), $r = 10$ (C) and $r = 100$ (D).

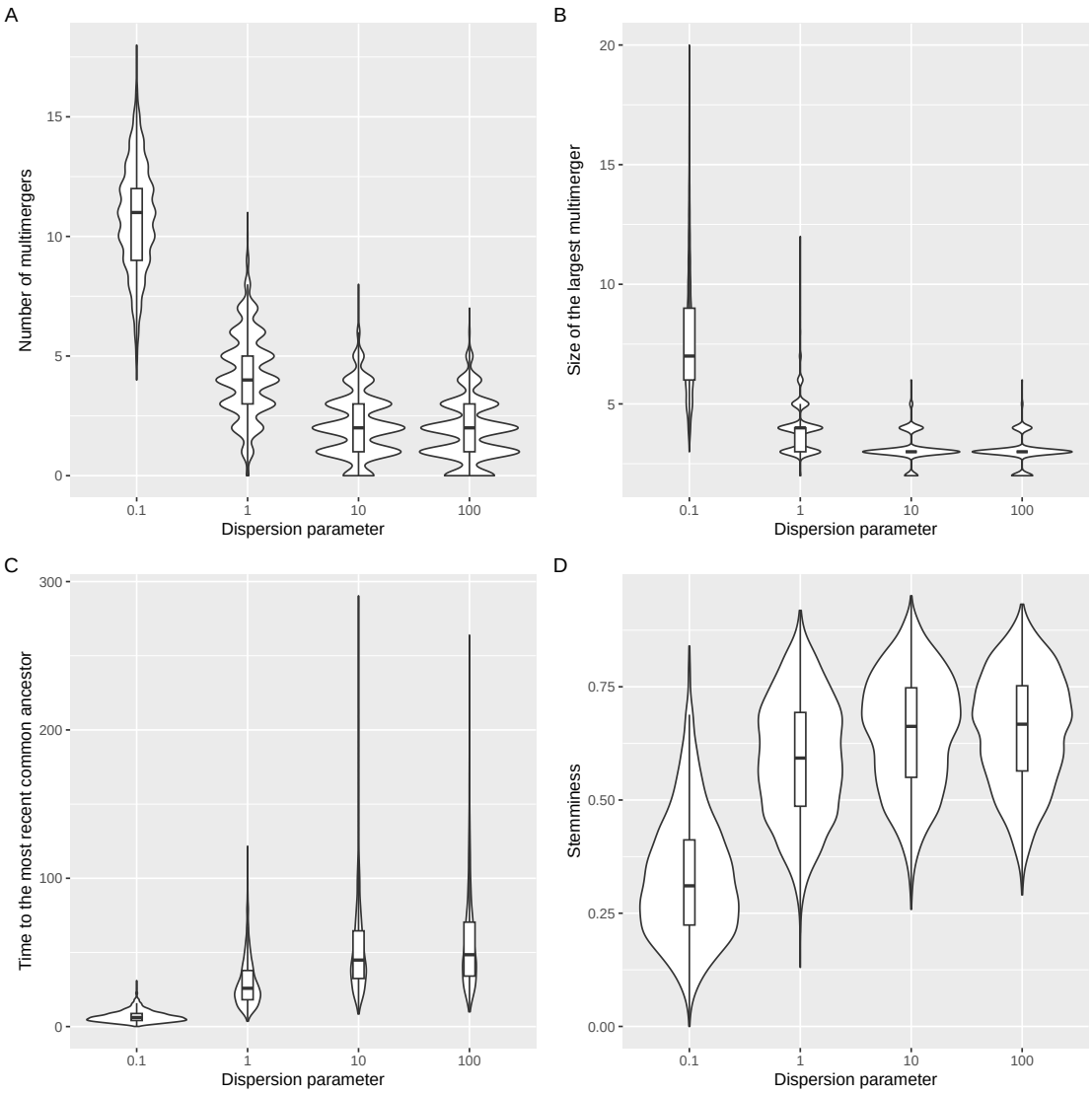

Figure 5: Summary statistics for trees simulated under the omega-coalescent with $r = 0.1$, $r = 1$, $r = 10$ and $r = 100$, namely number of multimergers (A) the size of the largest multimerger (B), the time to the most recent common ancestor (C) and the stemminess (D).

a lambda-coalescent model, the genealogy T has likelihood:

$$p(T|\Lambda) = \prod_{i=1}^{c} \lambda_{n_i,k_i} \exp\left(-\sum_{j=2}^{n_i} \binom{n_i}{j} \lambda_{n_i,j}(t_i - t_{i-1}) \right) \tag{31}$$

Note that in Equation 31 the term $\binom{n_i}{k_i}$ term from the coalescent rate cancels out with its reciprocal from the probability of sampling k_i specific lineages to coalesce within a set of n_i. Estimating the lambda measure from Equation 26 in general is a difficult problem (Koskela 2018; Miró Pina et al. 2023). Here however we focus on estimation under the omega-coalescent model, where the $\lambda_{n,k}$ terms are given by Equation 29. There are therefore two parameters to estimate which have direct and important biological meaning: the effective population size N_t (which remains constant) and the dispersion parameter r of the Negative-Binomial offspring distribution. We perform estimation simply by maximising the likelihood in Equation 31, using the Brent algorithm (Brent 1971) when estimating a single parameter and the L-BFGS-B algorithm (Byrd et al. 1995) when estimating both parameters.

We simulated 100 genealogies from the omega-coalescent model each of which had $n = 100$ leaves, with parameter N_t drawn uniformly at random between 100 and 500 and parameter r drawn uniformly at random between 0.01 and 2. If we assume knowledge of the dispersion parameter, then estimating the population size works really well (Figure 6A). Conversely we obtain good result when estimating the dispersion parameter given a known population size (Figure 6B). However, attempting to estimate both parameters at the same time performed significantly less well (Figures 6C and D). To illustrate the cause of this, we consider a simulation for which the true parameters were $N_t = 200$ and $r = 0.5$, and we construct the likelihood surface (Figure 6E). This shows a strong inverse tradeoff between the two parameters, which is why it is harder to infer both parameters jointly.

8 Implementation

We implemented the analytical methods described in this paper in a new R package entitled *EpiLambda* which is available at `https://github.com/xavierdidelot/EpiLambda` for R version 3.5 or later. All code and data needed to replicate the results are included in the "run" directory of the *EpiLambda* repository. The R package `ape` was used to store, manipulate and visualise phylogenetic trees (Paradis and Schliep 2019).

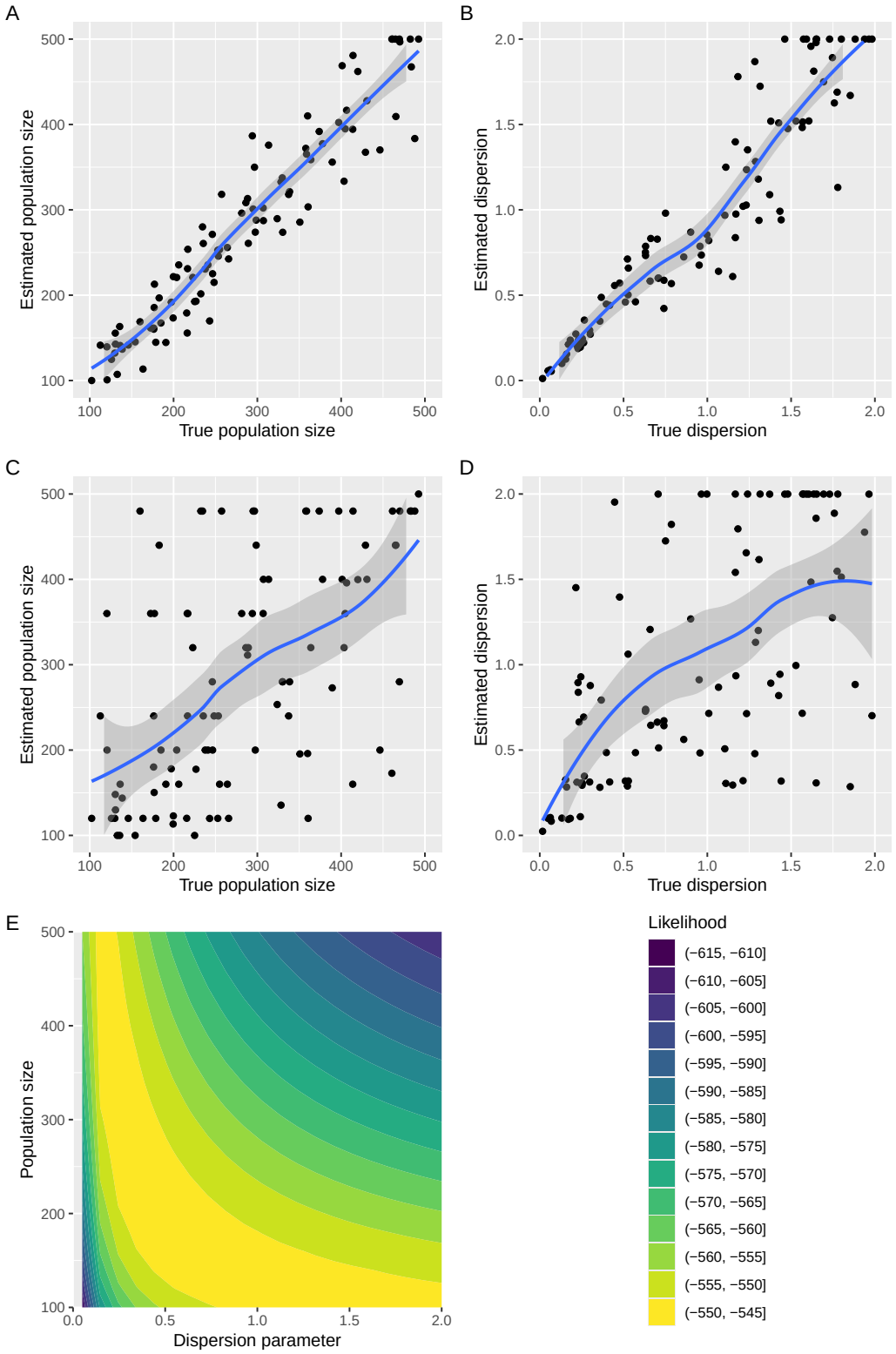

Figure 6: Maximum likelihood estimation of parameters. (A) Estimation of the population size given the dispersion parameter. (B) Estimation of the dispersion parameter given the population size. (C and D) Joint estimation of both the population size and dispersion parameters. (E) Example of likelihood surface as a function of both parameters.

9 Discussion

We have described an ancestral process for infectious diseases which is relevant to analysis of outbreaks of a relatively small size, and to diseases with high transmission heterogeneity. This process can be incorporated into a new lambda-coalescent which we called the omega-coalescent. We only considered the situation where all samples are taken at the same time, but the omega-coalescent could be extended to allow temporally offset leaves following similar work on the coalescent (Drummond et al. 2003) and the beta-coalescent (Hoscheit and Pybus 2019). We also made the simplifying assumption of a constant population size, but this could be relaxed following the same approach as previously described for integrating variable population size into the coalescent (Griffiths and Tavare 1994; Pybus et al. 2000; Ho and Shapiro 2011) and the beta-coalescent (Hoscheit and Pybus 2019; Zhang and Palacios 2024). Allowing the population size to vary could be especially useful for the omega-coalescent for several reasons. Firstly, since it is aimed at relatively small outbreaks, it is likely that their sizes varies significantly. Secondly, the probability of multimerger events of various sizes depends explicitly on the population size in Equation 21. Changes in population size will therefore have an effect on the distribution of events observed, as can be seen for example in Figure 3. Thirdly, joint inference of a varying population size could help break the otherwise difficult joint inference of a fixed population size with the dispersion parameter (Figure 6).

We compared the omega-coalescent only to the beta-coalescent (Schweinsberg 2003) in Figure 3 as it is the model that has been most frequently used for infectious diseases (Hoscheit and Pybus 2019; Menardo et al. 2021; Helekal et al. 2025). Several other lambda-coalescent models have been proposed previously, such as the Dirac coalescent (Eldon and Wakeley 2006), the Durrett-Schweinsberg coalescent (Durrett and Schweinsberg 2005) or the extended Beta-coalescent (Helekal et al. 2025). However, none of these models is equivalent to the omega-coalescent model. Indeed these previously described lambda-coalescent model are mostly concerned with situations where an individual can be the father of a significant portion of a population in spite of the population being large, rather than small populations with superspreading as we modelled here. The xi-coalescent models are extensions to the lambda-coalescent models that admit multiple simultaneous mergers (Schweinsberg 2000). This is clearly relevant to our basic discrete time model for small outbreaks, since in small populations it is quite likely that separate subsets of individuals have the same infector in the previous generation. However the exact timing of ancestry events is never available so that we must rely on ancestral dating estimation with no notion of event co-occurrence (Volz and Frost 2017; Didelot et al. 2018; Bouckaert et al. 2019; Helekal et al. 2025). Instead we introduced a continuous time approximation in Equation

29 so that ancestry events do not co-occur.

Finally, it should be noted that our model describes the transmission tree during an outbreak, which is different from a phylogeny (Jombart et al. 2011). This difference is often ignored and in some settings it might be appropriate to do so, but not always. Consequently, some previous studies have used models of within-host evolution to bridge the gap between transmission and phylogenetic trees (Didelot et al. 2014; Hall et al. 2015; Didelot et al. 2017). However, these models assume that each transmission event happens independently from one infector to each of its infectees. This is not necessarily true especially when considering superspreading events in which many individuals can become infected simultaneously (Riley et al. 2003; Wallinga and Teunis 2004; Ho et al. 2023). In conclusion, we have described a new ancestral model for infectious disease outbreak, which we hope will be useful especially in settings where the outbreaks are small or in the presence of high transmission heterogeneity.

Acknowledgements

We acknowledge funding from the National Institute for Health Research (NIHR) Health Protection Research Unit in Genomics and Enabling Data.

References

Anderson, R.M., May, R.M., 1991. Infectious Diseases of Humans: Dynamics and Control. Oxford University Press, USA.

Bouckaert, R., Vaughan, T.G., Fourment, M., Gavryushkina, A., Heled, J., Denise, K., Maio, N.D., Matschiner, M., Ogilvie, H., Plessis, L., Popinga, A., 2019. BEAST 2.5 : An Advanced Software Platform for Bayesian Evolutionary Analysis. PLoS computational biology 15, e1006650.

Brent, R.P., 1971. An algorithm with guaranteed convergence for finding a zero of a function. The computer journal 14, 422–425.

Byrd, R.H., Lu, P., Nocedal, J., Zhu, C., 1995. A limited memory algorithm for bound constrained optimization. SIAM Journal on scientific computing 16, 1190–1208.

Cannings, C., 1974. The latent roots of certain Markov chains arising in genetics: a new approach, I. Haploid models. Adv. Appl. Probab. 6, 260–290.

Didelot, X., Croucher, N.J., Bentley, S.D., Harris, S.R., Wilson, D.J., 2018. Bayesian inference of ancestral dates on bacterial phylogenetic trees. Nucleic Acids Research 46, e134–e134.

Didelot, X., Fraser, C., Gardy, J., Colijn, C., 2017. Genomic infectious disease epidemiology in partially sampled and ongoing outbreaks. Molecular Biology and Evolution 34, 997–1007.

Didelot, X., Gardy, J., Colijn, C., 2014. Bayesian inference of infectious disease transmission from whole genome sequence data. Molecular Biology and Evolution 31, 1869–1879.

Didelot, X., Urwin, R., Maiden, M.C.J., Falush, D., 2009. Genealogical typing of Neisseria meningitidis. Microbiology 155, 3176–86.

Donnelly, P., Kurtz, T.G., 1999. Particle Representations for Measure-Valued Population Models. The Annals of Probability 27.

Drummond, A.J., Pybus, O.G., Rambaut, A., Forsberg, R., Rodrigo, A.G., 2003. Measurably evolving populations. Trends in Ecology and Evolution 18, 481–488.

Du, Z., Wang, C., Liu, C., Bai, Y., Pei, S., Adam, D.C., Wang, L., Wu, P., Lau, E.H.Y., Cowling, B.J., 2022. Systematic review and meta-analyses of superspreading of SARS-CoV-2 infections. Transboundary and Emerging Diseases 69.

Durrett, R., Schweinsberg, J., 2005. A coalescent model for the effect of advantageous mutations on the genealogy of a population. Stochastic Processes and their Applications 115, 1628–1657.

Eldon, B., Wakeley, J., 2006. Coalescent Processes When the Distribution of Offspring Number Among Individuals Is Highly Skewed. Genetics 172, 2621–2633.

Ferguson, N.M., Cummings, D.A.T., Fraser, C., Cajka, J.C., Cooley, P.C., Burke, D.S., 2006. Strategies for mitigating an influenza pandemic. Nature 442, 448–452.

Fiala, K.L., Sokal, R.R., 1985. Factors determining the accuracy of cladogram estimation: Evoluation using computer simulation. Evolution 39, 609–622.

Fisher, R.A., 1930. The genetical theory of natural selection. Clarendon Press.

Fraser, C., Li, L.M., 2017. Coalescent models for populations with time-varying population sizes and arbitrary offspring distributions. bioRxiv , 10.1101/131730.

Fraser, C., Riley, S., Anderson, R.M., Ferguson, N.M., 2004. Factors that make an infectious disease outbreak controllable. Proceedings of the National Academy of Sciences 101, 6146–6151.

Gómez-Carballa, A., Pardo-Seco, J., Bello, X., Martinón-Torres, F., Salas, A., 2021. Superspreading in the emergence of COVID-19 variants. Trends in Genetics 37, 1069–1080.

Grassly, N.C., Fraser, C., 2008. Mathematical models of infectious disease transmission. Nature Reviews Microbiology 6, 477–87.

Griffiths, RC., Tavare, S., 1994. Sampling theory for neutral alleles in a varying environment. Philosophical Transactions of the Royal Society B 344, 403–410.

Hall, M., Woolhouse, M., Rambaut, A., 2015. Epidemic Reconstruction in a Phylogenetics Framework: Transmission Trees as Partitions of the Node Set. PLOS Computational Biology 11, e1004613.

Helekal, D., Koskela, J., Didelot, X., 2025. Inference of multiple mergers while dating a pathogen phylogeny. Systematic Biology , in press.

Ho, F., Parag, K.V., Adam, D.C., Lau, E.H.Y., Cowling, B.J., Tsang, T.K., 2023. Accounting for the Potential of Overdispersion in Estimation of the Time-varying Reproduction Number. Epidemiology 34, 201–205.

Ho, S.Y.W., Shapiro, B., 2011. Skyline-plot methods for estimating demographic history from nucleotide sequences. Molecular Ecology Resources 11, 423–434.

Hoscheit, P., Pybus, O.G., 2019. The multifurcating skyline plot. Virus Evolution 5, 1–10.

Jombart, T., Eggo, R.M., Dodd, P.J., Balloux, F., 2011. Reconstructing disease outbreaks from genetic data: A graph approach. Heredity 106, 383–90.

Keeling, M.J., Rohani, P., 2008. Modeling infectious diseases in humans and animals. Princeton university press.

Kingman, J., 1982a. The coalescent. Stochastic Processes and their Applications 13, 235–248.

Kingman, J.F.C., 1982b. On the genealogy of large populations. Journal of Applied Probability 19, 27–43.

Koelle, K., Rasmussen, D.A., 2012. Rates of coalescence for common epidemiological models at equilibrium. Journal of The Royal Society Interface 9, 997–1007.

Koskela, J., 2018. Multi-locus data distinguishes between population growth and multiple merger coalescents. Statistical Applications in Genetics and Molecular Biology 17, 1–24.

Kucharski, A.J., Althaus, C.L., 2015. The role of superspreading in Middle East respiratory syndrome coronavirus (MERS-CoV) transmission. Eurosurveillance 20.

Lemieux, J.E., Siddle, K.J., Shaw, B.M., Loreth, C., Schaffner, S.F., Gladden-Young, A., Adams, G., Fink, T., Tomkins-Tinch, C.H., Krasilnikova, L.A., DeRuff, K.C., Rudy, M., Bauer, M.R., Lagerborg, K.A., Normandin, E., Chapman, S.B., Reilly, S.K., Anahtar, M.N., Lin, A.E., Carter, A., Myhrvold, C., Kemball, M.E., Chaluvadi, S., Cusick, C., Flowers, K., Neumann, A., Cerrato, F., Farhat, M., Slater, D., Harris, J.B., Branda, J.A., Hooper, D., Gaeta, J.M., Baggett, T.P., O'Connell, J., Gnirke, A., Lieberman, T.D., Philippakis, A., Burns, M., Brown, C.M., Luban, J., Ryan, E.T., Turbett, S.E., LaRocque, R.C., Hanage, W.P., Gallagher, G.R., Madoff, L.C., Smole, S., Pierce, V.M., Rosenberg, E., Sabeti, P.C., Park, D.J., MacInnis, B.L., 2021. Phylogenetic analysis of SARS-CoV-2 in Boston highlights the impact of superspreading events. Science 371, eabe3261.

Li, L.M., Grassly, N.C., Fraser, C., 2017. Quantifying Transmission Heterogeneity Using Both Pathogen Phylogenies and Incidence Time Series. Molecular Biology and Evolution 34, 2982–2995.

Lloyd-Smith, J., Schreiber, S., Kopp, P., Getz, W., 2005. Superspreading and the effect of individual variation on disease emergence. Nature 438, 355–9.

Menardo, F., Gagneux, S., Freund, F., 2021. Multiple Merger Genealogies in Outbreaks of Mycobacterium tuberculosis. Molecular Biology and Evolution 38, 290–306.

Miró Pina, V., Joly, É., Siri-Jégousse, A., 2023. Estimating the Lambda measure in multiple-merger coalescents. Theoretical Population Biology 154, 94–101.

Moran, P., 1958. Random Processes in Genetics. Mathematical Proceedings of the Cambridge Philosophical Society 54, 60–71.

Paradis, E., Schliep, K., 2019. Ape 5.0: An environment for modern phylogenetics and evolutionary analyses in R. Bioinformatics 35, 526–528.

Pitman, J., 1999. Coalescents with multiple collisions. The Annals of Probability 27, 1870–1902.

Potts, R.B., 1953. Note on the Factorial Moments of Standard Distributions. Australian Journal of Physics 6, 498–499. Publisher: CSIRO PUBLISHING.

Pybus, O.G., Rambaut, A., Harvey, P.H., 2000. An integrated framework for the inference of viral population history from reconstructed genealogies. Genetics 155, 1429–1437.

Riley, S., Fraser, C., a Donnelly, C., Ghani, A.C., Abu-Raddad, L.J., Hedley, A.J., Leung, G.M., Ho, L.M., Lam, T.H., Thach, T.Q., Chau, P., Chan, K.P., Lo, S.V., Leung, P.Y., Tsang, T., Ho, W., Lee, K.H., Lau, E.M.C., Ferguson, N.M., Anderson, R.M., 2003. Transmission dynamics of the etiological agent of SARS in Hong Kong: Impact of public health interventions. Science 300, 1961–6.

Sagitov, S., 1999. The general coalescent with asynchronous mergers of ancestral lines. Journal of Applied Probability 36, 1116–1125.

Schweinsberg, J., 2000. Coalescents with Simultaneous Multiple Collisions. Electronic Journal of Probability 5.

Schweinsberg, J., 2003. Coalescent processes obtained from supercritical Galton–Watson processes. Stochastic Processes and their Applications 106, 107–139.

Stein, R.A., 2011. Super-spreaders in infectious diseases. International Journal of Infectious Diseases 15, e510–e513.

Svensson, A., 2007. A note on generation times in epidemic models. Mathematical Biosciences 208(1), 300–311.

Tripathi, R.C., Gupta, R.C., Gurland, J., 1994. Estimation of parameters in the beta binomial model. Annals of the Institute of Statistical Mathematics 46, 317–331.

Volz, E.M., 2012. Complex population dynamics and the coalescent under neutrality. Genetics 190, 187–201.

Volz, E.M., Frost, S.D.W., 2017. Scalable relaxed clock phylogenetic dating. Virus Evolution 3, vex025.

Wallinga, J., Teunis, P., 2004. Different Epidemic Curves for Severe Acute Respiratory Syndrome Reveal Similar Impacts of Control Measures. American Journal of Epidemiology 160, 509–516.

Wang, J., Chen, X., Guo, Z., Zhao, S., Huang, Z., Zhuang, Z., Wong, E.L.y., Zee, B.C.Y., Chong, M.K.C., Wang, M.H., Yeoh, E.K., 2021. Superspreading and heterogeneity in transmission of SARS, MERS, and COVID-19: A systematic review. Computational and Structural Biotechnology Journal 19, 5039–5046.

Wang, L., Didelot, X., Yang, J., Wong, G., Shi, Y., Liu, W., Gao, G.F., Bi, Y., 2020. Inference of person-to-person transmission of COVID-19 reveals hidden super-spreading events during the early outbreak phase. Nature Communications 11, 5006.

Woolhouse, M.E.J., Dye, C., Etard, J.F., Smith, T., Charlwood, J.D., Garnett, G.P., Hagan, P., Hii, J.L.K., Ndhlovu, P.D., Quinnell, R.J., Watts, C.H., Chandiwana, S.K., Anderson, R.M., 1997. Heterogeneities in the transmission of infectious agents: Implications for the design of control programs. Proceedings of the National Academy of Sciences 94, 338–342.

Wright, S., 1931. Evolution in Mendelian populations. Genetics 16, 97–159.

Zhang, J., Palacios, J.A., 2024. Multiple merger coalescent inference of effective population size. arXiv , 2407.14976.